

Adaptive Robust MPPT for a Perturbed PV System with Experimental Verification

Marjan Faghih
MSc student
Department of Electrical
Engineering
University of Isfahan
Isfahan, Iran, 8174673441
Email: m.faghih@eng.ui.ac.ir

Hamidreza Koofgar
Assistant professor
Department of Electrical
Engineering
University of Isfahan
Isfahan, Iran, 8174673441
Email: koofgar@eng.ui.ac.ir

Behzad Mirzaeian Dehkordy
Associate professor
Department of Electrical
Engineering
University of Isfahan
Isfahan, Iran, 8174673441
Email: mirzaeian@eng.ui.ac.ir

Abstract—In this paper, a sliding surface is defined based on the inductor current to construct robust controller for Maximum Power Point Tracking (MPPT) in photovoltaic (PV) systems. An adaptive incremental conductance algorithm have been used to obtain the set point of the controller. An improvement is achieved by this combination, especially in fast irradiance variations. The robust stability of the method is proved using the Lyapunov stability theorem. A comparative study is also made to highlight the benefits of the proposed algorithm. The features of this controller, in terms of robustness against the irradiance variations, are demonstrated by theoretical analysis, simulations and an experimental study. The results demonstrate that the proposed controller can be implemented effectively and economically with high MPPT efficiency.

Keywords—maximum power point tracking; photovoltaic system; sliding mode controller; DC-DC converter.

I. INTRODUCTION

Renewable energy resources such as solar, wind and sea wave are some alternatives for fossil-fuel energy sources. Among all these resources, solar energy attracts more attention these days, because it is much clean, has capability to use in movable systems, free and easy to harvest in every place of the earth and inexhaustible [1].

Every photovoltaic module has a nonlinear current-voltage diagram and power-voltage characteristic with an optimal operating point, named maximum power point (MPP). This point varies over a wide range with variation of PV module's temperature and solar irradiation. Therefore, in order to operate at MPP, the electrical characteristics of load should vary by a time varying matching network. The task of this network, called MPPT, is to ensure operation of the PV at its MPP in the presence of temperature and irradiance variations. Normally, this network implemented by means of a DC-DC converter that controlled by its duty cycle [2].

Many methods that have been developed vary in complexity, number of sensors required, convergence time, cost, range of effectiveness, simplicity in implementation, popularity and etc. [3]. Among these methods hill-climbing [4], and perturb and observed [5] were commonly used due to

their straight forward and economically implementation. In these two methods by perturbing duty cycle (or voltage and current) then observing output power gives good information for adjusting duty cycle. Incremental conductance [6] is an alternative method, which acts base on the fact that power curve's slope is positive at left, negative at right, and zero at MPP [7]. However, all these methods did not operate well during rapidly change in atmosphere condition and persist of uncertainty in system parameters.

Sliding Mode Control (SMC) is a robust method against both internal parameters uncertainties and external disturbances. Therefore, with the right choice of sliding surface as PV voltage or current, a fast and robust method could replace conventional methods.

For the fast MPPT, the linear dependency of PV current against irradiance could be used, but the rapidly change of irradiance might lead to failure in control operation [9]. Recently, two control loops have been proposed to overcome this problem. The first loop finds the voltage in the MPP by an MPPT algorithm, and a sliding mode controller in the second loop tracks that point, based on current [2, 8-10].

In this paper, an adaptive incremental conductance used to find the MPP voltage, then a sliding mode controller base on inductor current used that point to track the MPP. A temperature sensor has been used due to converting voltage set point to reference current for sliding mode controller. Then by the aim of that temperature, PV current and voltage the real irradiance calculated by current relation of PV. In recent studies to do this converting, a PI controller has been used, which is not accurate and lead to decrease the MPPT efficiency [8, 10]. Robust analysis done because of uncertainty in system parameters due to passive component. An unknown uncertainty bound has been considered and its upper bound has been calculated by an adaption law. Compared with traditional MPPT methods, the proposed method take less time to settle at MPP, eliminate oscillation around operating point, increased MPP efficiency, and robust against disturbances, uncertainties of system parameters and fast change in atmosphere conditions.

This paper is organized as follows: In section II, the electric characteristics of PV is described. Modeling of MPPT system is discussed in section III. The proposed controller came in section IV, which consist of MPP algorithm and sliding mode part of controller. In section V the robustness issue of the proposed method is presented. Simulation and experimental results are given in sections VI and VII, respectively. Conclusion is addressed in last section.

II. PV CHARACTERISTICS

Solar cell is a P-N junction that convert solar light to electrical power. Each solar module constructed by several solar cells that connected in series and parallel to generate required power. For obtaining more power, solar PV module connected in series and parallel to form solar PV arrays [11]. The equivalent circuit model of a solar cell consists of a light generated current source, diode and series and parallel resistances. To simplify the model, the parallel resistor may be neglected in the equations. The mathematical expressions of the model is given by

$$I = I_{ph} - I_d \left[\exp\left(\frac{q}{KTA}(V + R_s)\right) - 1 \right] \quad (1)$$

$$I_{ph} = S[I_{scr} + K_i(T - T_r)]$$

$$I_d = I_{rr} \left[\frac{T}{T_r} \right]^3 \cdot \exp\left(\frac{qE_g}{kQA} \left[\frac{1}{T_r} - \frac{1}{T} \right] \right)$$

Also, the description of each parameter in these equations is presented in Table 1 [12].

TABLE I. PARAMETER EXPRESSION OF SOLAR CELL EQUATION.

Parameter	Expression	Parameter	Expression
I	PV output current (A)	I_{scr}	Short circuit current at reference condition
V	PV output voltage (V)	T_r	Reference
T	Cell temperature (K)	K_i	Short circuit temperature coefficient
S	Solar irradiance (W/m^2)	q	Charge of an electron
R_s	Series resistor (Ω)	K	Boltzmann's constant
I_{ph}	Light generated current	E_g	Band-gap energy of the material
I_d	PV saturation current	Q	Total electron charge
I_{rr}	Saturation current at T_r	A	Ideality factor

The current-voltage characteristic diagram is plotted in Fig. 1, under various irradiances and a constant temperature (25°C). The variations in the irradiance affect the short-circuit current (I_{sc}), while temperature dominated on open-circuit voltage (V_{oc}). Therefore, one concludes that the increase in irradiance and decrease in the temperature cause increase in output power of PV [13].

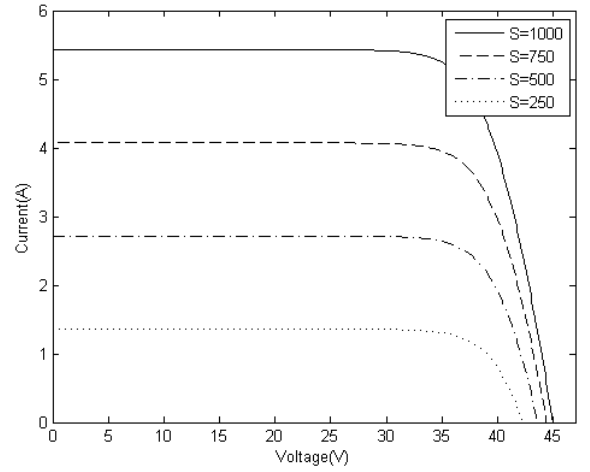


Figure 1. PV characteristics under different irradiance level (Temperature=25°C)

III. MODELING OF MPPT SYSTEM

In order to maximize the PV power a DC-DC boost converter has been used, the construction of such system shown in Fig. 2. In the following, the boost converter is used in the continuous current mode (CCM), which means that the inductor current never falls to zero. The resulting state space description is obtained by the averaging method as [14]:

$$\begin{aligned} \dot{V}_{pv} &= \frac{1}{C_1}(I_{pv} - i_L) \\ \dot{i}_L &= \frac{V_{pv}}{L} - \frac{V_o}{L} + \frac{V_o}{L}d \\ \dot{V}_o &= \frac{i_L}{C_2} + \frac{V_o}{C_2 R_L} - \frac{i_L}{C_2}d \end{aligned} \quad (2)$$

where, V_{pv} , I_{pv} and V_o , I_o are voltage and current of input and output of converter, respectively, C_1 and C_2 are respectively input and output capacitors, L is inductor, i_L is inductor's current, R_L is output resistive load and finally d is the duty cycle and control input of the system.

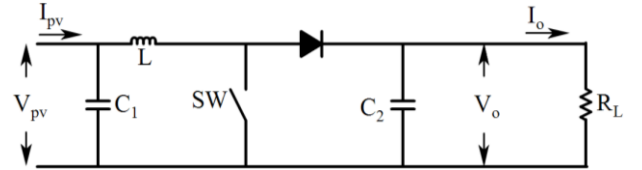


Figure 2. Boost converter circuit.

IV. MPPT PROPOSED TECHNIQUE

In order to find MPP under varying atmosphere condition and system uncertainties, overall structure of fig.3 have been proposed. Searching algorithm find reference voltage in each time by the use of PV voltage and current, then, with this voltage and temperature from the temperature sensor the reference current will be obtained. Proportional to the current situation of system the duty cycle may be obtained and applied to the boost converter switch.

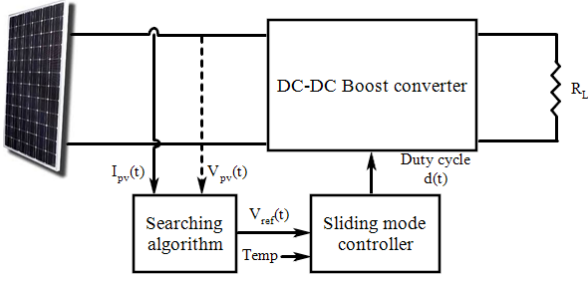


Figure 3. MPPT structure by two control loop.

A. MPP searching algorithm

To find MPP we use an incremental conductance with an adaptive step size. Base on power relation and its slop

$$P_{pv} = V_{pv} \times I_{pv} \quad (3)$$

$$\frac{\partial P_{pv}}{\partial V_{pv}} = I_{pv} + V_{pv} \frac{\partial I_{pv}}{\partial V_{pv}} \quad (4)$$

When the power slop became zero, (i.e. $\frac{\partial I_{pv}}{\partial V_{pv}} = -\frac{I_{pv}}{V_{pv}}$) the

system will work on MPP. Choose big step sizes lead to decrease convergence time, while in steady state some oscillations will appear on output. In order to tackle this problem we could use an adaptive step size. Finally, the updating law is written as:

$$\begin{cases} V_{ref}(t) = V_{ref}(t-1) + \Delta V_{ref}(t), \text{ for } \frac{\partial I_{pv}}{\partial V_{pv}} > -\frac{I_{pv}}{V_{pv}} \\ V_{ref}(t) = V_{ref}(t-1) - \Delta V_{ref}(t), \text{ for } \frac{\partial I_{pv}}{\partial V_{pv}} < -\frac{I_{pv}}{V_{pv}} \end{cases} \quad (5)$$

where V_{ref} is reference voltage and $\Delta V_{ref}(t)$ is an adaptive step size

$$e = \Delta I / \Delta V + I/V \quad (6)$$

$$\Delta V_{ref}(t) = \alpha \times e \quad (7)$$

where, $\Delta I = I(t) - I(t-1)$ and $\Delta V = V(t) - V(t-1)$ and α is a positive constant, chosen by trial and error, which should be chosen to not being more than the open circuit voltage of solar module in big errors.

B. Sliding mode controller

Sliding surface for this controller chosen like (8). Reference Voltage could simply convert to reference current by (1), then by (2) the inductor reference current could be obtained.

$$S = I_L - I_{Lref} \quad (8)$$

The next step is to design a sliding surface, which satisfied the existence law. The control input could have following structure:

$$d(t) = d_{eq}(t) + d_n(t) \quad (9)$$

where, $d_{eq}(t)$ is an equivalent control input that determines behavior of the system on the sliding surface. It obtained in situation that sliding surface is equal to zero. Then we have:

$$d_{eq} = \frac{L}{V_o} \dot{I}_{Lref} + \frac{V_o - V_{pv}}{V_o} \quad (10)$$

To drive and maintain state on the sliding surface in the presence of the parameter variations and disturbances a nonlinear switching control input is required, which named $d_n(t)$ [14]. It could be chosen like $d_n(t) = -K \text{sign}(S)$, where K is a constant that chose by trial and error proportional to the output response. In order to reduce steady state chattering of output it can be chosen as [15]:

$$d_n = -K \text{sat}(S) \quad (11)$$

V. ROBUSTNESS ANALYSIS

Due to system uncertainty, measurement errors, passivity of components and also variation in atmosphere conditions an uncertainty term named Δ could be considered. Generally this uncertainty show itself on input current, therefore it is better to add Δ term to inductor current among other state variables.

$$\dot{I}_L = \frac{V_{pv}}{L} - \frac{V_o}{L} + \frac{V_o}{L} d + \Delta \quad (12)$$

where, Δ is an unknown uncertainty that its bound will be estimated by an adaptive law during controller design. Sliding surface will chose like last section. The control input could be chosen as:

$$d(t) = d_{eq}(t) + d_n(t) + \alpha S(t) \quad (13)$$

By differentiation of sliding surface and substituting on (13) we have

$$\dot{S} = \frac{V_{pv}}{L} - \frac{V_o}{L} + \frac{V_o}{L} \left(\frac{L}{V_o} \dot{I}_{Lref} + \frac{V_o - V_{pv}}{V_o} \right) \quad (14)$$

$$-K \text{sign}(\gamma S) + \alpha S + \Delta - \dot{I}_{Lref}$$

$$\dot{S} = \alpha \frac{V_o}{L} S - \beta \frac{V_o}{L} \text{sign}(\gamma S) + \Delta \quad (15)$$

Now, by defining a proper positive definite Lyapunov function candidate, we tried to negative definite its derivative.

$$V = \frac{1}{2} S^2 + \frac{1}{2} \delta \tilde{D}^2 \quad (16)$$

where, $\tilde{D} = D - \hat{D}$ and δ is a positive constant. Differentiation of Lyapunov function is $\dot{V} = S \dot{S} + \delta \tilde{D} \dot{\tilde{D}}$, by considering low variation for D , $\dot{\tilde{D}} = \dot{\hat{D}}$ therefor:

$$\alpha \frac{V_o}{L} S^2 - \beta S \frac{V_o}{L} \text{sign}(\gamma S) + |S| |\Delta| + \delta (D - \hat{D}) (\dot{\hat{D}}) \leq 0 \quad (17)$$

In case, we choose $-\beta S \frac{V_o}{L} \text{sign}(\gamma S) + |S| |\Delta| + \delta (D - \hat{D}) (\dot{\hat{D}}) = 0$

and $\alpha = -\varepsilon \frac{L}{V_o}$, therefore $\dot{V} = -\varepsilon S^2$ that if we choose $\varepsilon > 0$,

will get into $\dot{V} \leq 0$. To confirm (19) it is necessary to $\beta = \hat{D}$ and $\gamma = \frac{V_o}{L}$, hence

$$(D - \hat{D})(|S| - \delta \dot{\hat{D}}) = 0 \quad (18)$$

By utilizing (18) adaption law for estimate of uncertainty upper bound yield [16]:

$$\dot{\hat{D}} = \frac{1}{\delta} |S| \quad (19)$$

Increase estimate value of \hat{D} without any bound will cause instability in system. Projection algorithm that proposed here is an effective method to this problem [17]. Therefore, adaption law replace by:

$$\dot{\hat{D}} = \eta |S| \quad (20)$$

where

$$\eta = \begin{cases} \frac{1}{\delta}, & \text{for } |e| > \varepsilon \\ 0, & \text{Otherwise} \end{cases}$$

where, e is an error term, which can be sliding surface.

VI. SIMULATION RESULTS

Numerical simulation of proposed method has been done in MATLAB, which used parameters in Table II. In the study, STP185S-24/Adb+ monocrystalline solar module with 14.5% conversion efficiency have been used. Controller parameters are set to $K=0.1$ and $\alpha=8.5 \times 10^{-10}$. Meanwhile, a P&O controller with $\Delta V_{\text{ref}}=3 \times 10^{-5}$ as step size, has been applied to system to compare with proposed controller. Simulation results for constant irradiance ($1000\text{W}/\text{m}^2$) and temperature (25°C) of these two methods shown in fig.4 and 5. In order to show the capability of the proposed method in rapidly change of irradiance, Figs. 6 and 7 illustrate the tracking results of both methods while irradiance change from $1000\text{W}/\text{m}^2$ to $500\text{W}/\text{m}^2$ in $t=2\text{sec}$. The tracking time of proposed method is less than P&O and have no fluctuation around MPP, also because of the robustness of the proposed method it has capability of tracking MPP under varying condition.

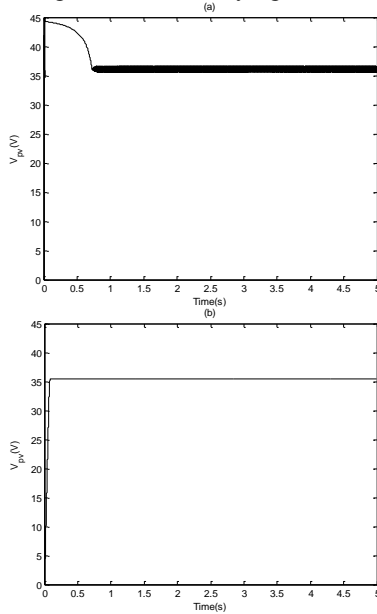


Figure 4. PV module voltage, (a) P&O controller, (b) proposed controller.

TABLE II. LIST OF PARAMETERS USED IN SIMULATION.

Parameter	Value	Parameter	Value
V_{oc}	45(V)	A	1.06
I_{sc}	5.43(A)	L	0.82(mH)
K	$1.3805 \times 10^{-23}(\text{J/K})$	C_1	470(μF)
q	$1.6 \times 10^{-19}(\text{C})$	C_2	1000(μF)
E_g	1.11(V)	R_L	68.8(Ω)
R_s	0.0088(Ω)	F_{sw}	31.3(KHz)

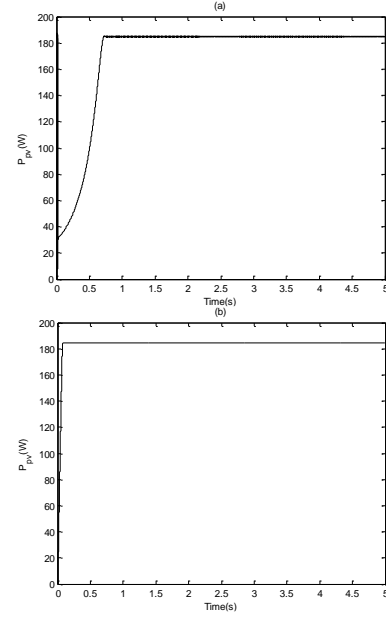


Figure 5. PV module power, (a) P&O controller, (b) proposed controller.

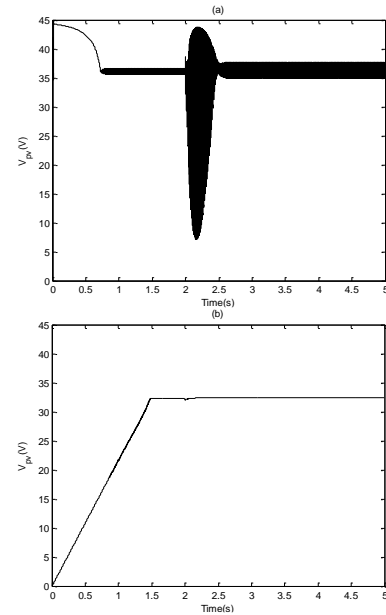


Figure 6. PV module voltage, (a) P&O controller, (b) proposed controller, in rapidly change of irradiance.

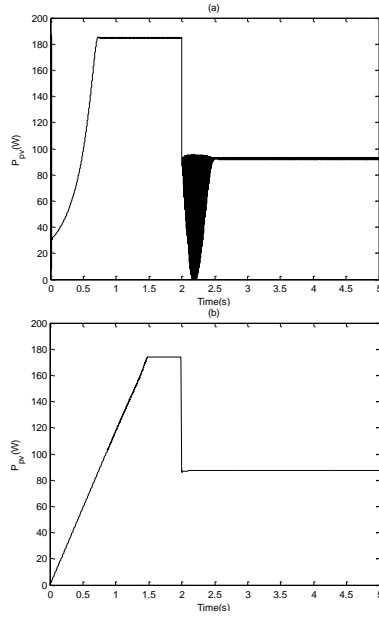


Figure 7. PV module power, (a) P&O controller, (b) proposed controller, in rapidly change of irradiance.

VII. EXPERIMENTAL RESULTS

In order to verify the effectiveness of proposed method, consider the configuration of experiment set up, as illustrated in Fig. 8. The proposed controller have been implemented on an AVR microcontroller (Atmega32), to control the duty cycle of MOSFET (IRFP264). The PV current measured by a current sensor (ASC712) and corresponding voltage of this current along with corresponding voltage from temperature sensor (LM335) and reduced PV voltage from resistive net inserted into microcontroller, which sampling time for ADC part is 400ms. After analyzing on the input data, the duty cycle with 31.3 KHz is obtained. A MOSFET driver (HCPL-3120) have been used to drive the power MOSFET with proper voltage.

The experiment have been conducted under irradiance of 485W/m^2 and module's temperature of 37°C . A heater as an output resistive load has been connected to the boost converter. The waveforms of proposed method illustrated in fig. 9. The results for P&O, in the same condition for the proposed method, are compared in Table III. As it can be seen MPPT efficiency of proposed method is more than P&O. This means that proposed method has more capability of tracking MPP. Utilizing a more efficient controller could increase efficiency and also decrease convergence time.

TABLE I. COMPARISON OF DIFFERENT METHODS OF MPPT.

Method	$V_{pv}(v)$	$I_{pv}(A)$	$V_o(v)$	$P_i(w)$	Efficiency (%)
Sliding mode	37.2	2.5	76.54	93	95.29
P&O	36.1	2.4	74.3	86.64	88.77
Open circuit	37.8	0.55	-	20.76	21.27

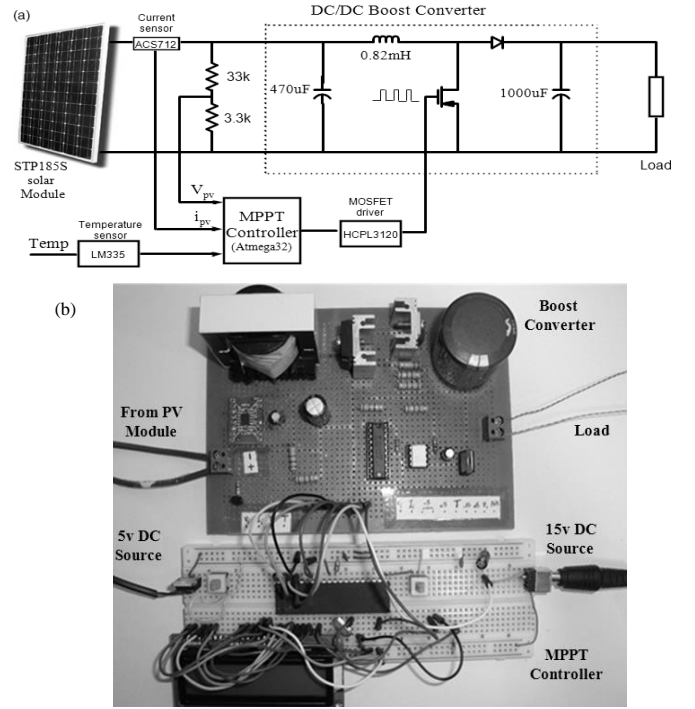


Figure 8. Configuration of experiment, (a) block diagram, (b) real picture.

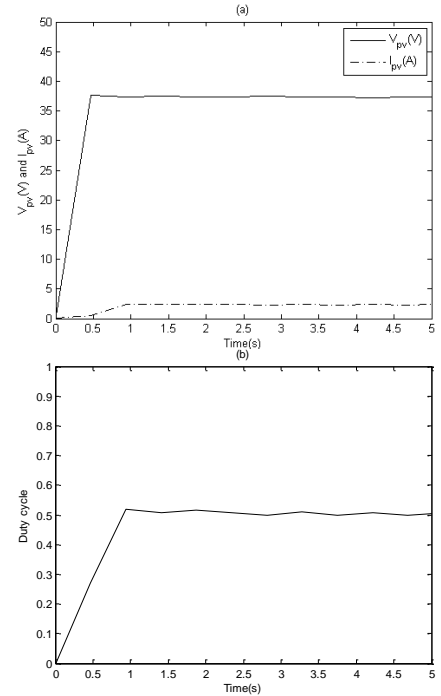


Figure 9. Implementation results, (a) PV voltage and current waveforms, (b) Duty cycle waveform.

VIII. CONCLUSION

In this paper, a sliding mode controller base on inductor current is considered. An improved MPPT searching algorithm along with a sliding mode controller proposed. This new algorithm show fast convergence time of finding MPP and well robustness under rapidly change of atmosphere condition. The experimental results confirm the simulation results and effectiveness of proposed method. This proposed method provides a feasible approach to harvesting solar energy from PV modules.

REFERENCES

- [1] M. A. A. M. Zainuri, M. A. M. Radzi, A. C. Soh, N. A. Rahim, "Development of adaptive perturb and observe-fuzzy control maximum power point tracking for photovoltaic boost dc-dc converter", *IET Renew. Power Gener.*, Vol. 8, Iss. 2, pp. 183–194, 2014.
- [2] Y. Levron and D. Shmilovitz, "Maximum power point tracking employing sliding mode control," *IEEE Trans. on Circ. and Sys.*, vol.60, no. 3, pp. 724–732, 2013.
- [3] T. Esum and P. Chapman, "Comparison of photovoltaic array maximum power point tracking techniques," *IEEE Trans. on Ene. Conv.*, vol. 22, no. 2, 2007.
- [4] E. Koutroulis, K. Kalaitzakis, N. C. Voulgaris, "Development of a microcontroller-based Photovoltaic maximum power point tracking control system", *IEEE Trans. Power Electron.*, vol. 16, pp. 46–54, 2001.
- [5] C. Hua, J. Lin, "An on-line MPPT algorithm for rapidly changing illuminations of solar arrays", *Renew. Energy*, vol. 28, pp. 1129–1142, 2003.
- [6] G. J. Yu, Y. S. Jung, J. Y. Choi, G. S. Kim, "A novel two-mode MPPT control algorithm based on comparative study of existing algorithms", *Sol. Energy*, vol. 76, pp. 455–463, 2004.
- [7] A. Reisi, M. Moradi, and S. Jamasb, "Classification and comparison of maximum power point tracking techniques for photovoltaic system: A review," *Renew. Sustain. Energy Rev.*, vol. 19, pp. 433–443, Mar. 2013.
- [8] E. Bianconi, J. Calvente, R. Giral, S. Member, E. Mamarelis, G. Petrone, C. A. Ramos-paja, G. Spagnuolo, and M. Vitelli, "A fast current-based MPPT technique employing sliding mode control," *IEEE Trans. on Ind. Electron.*, vol. 60, no. 3, pp. 1168–1178, 2013.
- [9] C. Chiu, Y. Ouyang, and C. Ku, "Terminal sliding mode control for maximum power point tracking of photovoltaic power generation systems," *Sol. Energy*, vol. 86, no. 10, pp. 2986–2995, 2012.
- [10] E. Bianconi, J. Calvente, R. Giral, E. Mamarelis, G. Petrone, C. A. Ramos-paja, G. Spagnuolo, and M. Vitelli, "Perturb and observe MPPT algorithm with a current controller based on the sliding mode," *Int. J. Electr. Power Energy Syst.*, vol. 44, no. 1, pp. 346–356, 2013.
- [11] M. EL-Moghany, "Sun and Maximum Power Point Tracking in Solar Array Systems Using Fuzzy Controllers Via FPGA," Master thesis 2011.
- [12] C. Chu and C. Chen, "Robust maximum power point tracking method for photovoltaic cells: A sliding mode control approach," *Sol. Energy*, vol. 83, no. 8, pp. 1370–1378, 2009.
- [13] R. Middlebrook and S. Cuk, "A general unified approach to modelling switching-converter power stages," *IEEE Power Electron. Spec. Conf.*, pp. 18–34, Jun. 1976.
- [14] S. Kim, "Sliding mode controller for the single-phase grid-connected photovoltaic system", *Applied Energy*, Vol. 83, Iss. 10, pp. 1101–1115, 2006.
- [15] J. J. E. Slotine, W. Li, "Applied Nonlinear Control", Prentice-Hall, Englewood Cliffs, New Jersey, 1991.
- [16] S. A. Zahiripour, A. A. Jalali, "Designing an adaptive sliding-mode controller for car active suspension system using an optimal proportional-integral sliding surface", *Int. Conf. on Future Inf. Tech. and Manag. Science & Eng.* Vol. 14, pp. 248–255, 2012.
- [17] H. R. Koofgar, "Robust adaptive motion control with environmental disturbance rejection for perturbed underwater vehicles", *Journal of Marine Science and Technology*, Vol. 22, No. 4, pp. 455–462, 2014.